

COMMUNICATION

Importance of steric bulkiness of iridium photocatalysts with PNNP tetradentate ligands for CO₂ reduction†

Received 00th January 20xx,
Accepted 00th January 20xx

Kenji Kamada,^a Jieun Jung,^{*a} Yohei Kametani,^b Taku Wakabayashi,^a Yoshihito Shiota,^b Kazunari Yoshizawa,^b Seong Hee Bae,^a Manami Muraki,^a Masayuki Naruto,^a Keita Sekizawa,^c Shunsuke Sato,^c Takeshi Morikawa^c and Susumu Saito^{*ad}

DOI: 10.1039/x0xx00000x

A series of Ir complexes has been developed as multifunctional photocatalysts for CO₂ reduction to give HCO₂H selectively. The catalytic activities and photophysical properties vary widely across the series, and the bulky group insertion resulted in the formation of HCO₂H and CO with the catalyst turnover number of > 10400.

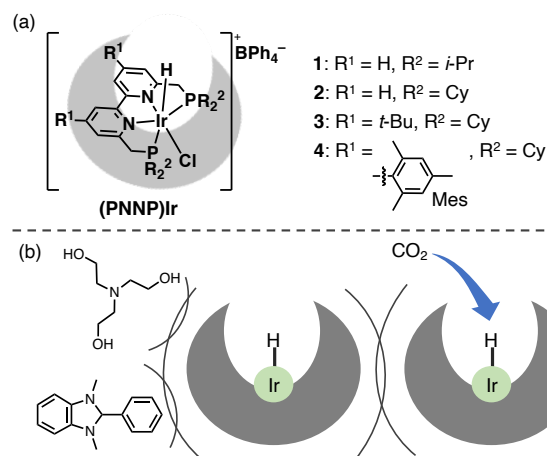
Activation and transformation of carbon dioxide (CO₂) have widely been investigated in an attempt to realize artificial photosynthesis, in which photoinduced electron transfer (ET) followed by catalytic CO₂ reduction is attracting extensive interest since the conversion of CO₂ to energy-rich compounds could occur under mild conditions, potentially without mandating the formation of salt waste.^{1,2} A two-component system involving a transition metal catalyst and a photosensitizer has been a typical approach to achieve stepwise multi-electron reduction of CO₂.^{3,4} A self-photosensitized, mononuclear (single metal-active-site) photocatalyst could mitigate the frequency of ET that may cause non-negligible energy loss. However, the development of a self-photosensitized catalyst with a high turnover number (TON) and quantum efficiency is still a significant challenge.⁵

Iridium (Ir) complexes, either working as a photosensitizer or a transition metal catalyst (the reduction site for CO₂), have thus far been a central interest due to their strong absorption in the visible-light region as well as remarkable properties to reduce CO₂.^{6,7} However, the reported Ir complexes showed catalyst degradation, probably due to the dimerization⁶ or reaction of a sacrificial electron donor with the ligand bound to the metal.⁸ Importance of substituent incorporation into an original ligand⁶ was implied to increase the TON.⁹

Our group has developed bidentate P,N- and tetradentate PNNP (6,6'-bis(phosphinomethyl)-2,2'-bipyridyl (bpy)) ligands of ruthenium (Ru) and Ir complexes as the catalysts for effective hydrogenation of unactivated amides^{10a,b} as well as

polycarboxylic acids.^{10c,d} The key to success is the highly stable PNNP-metal frameworks, which can tolerate harsh conditions and activation of C=O bonds of carboxyl groups with the bifunctional mechanism,¹¹ leading to efficient reductive catalytic reactions. Based on these results, we further reported structurally more robust, (PNNP)Ir^{12a} and (PNNP)Ru^{12b} complexes as efficient homogeneous photocatalysts for CO₂ reduction to give HCO₂H selectively under visible-light irradiation.

Herein, we systematically studied the relationship between metal complex substituents and catalytic activity/durability across a series of substituted (PNNP)Ir complexes (Scheme 1), in which steric factors of bulky substituents, rather than their electronic factors, are manifested in the most efficient photocatalytic CO₂ reduction, by clarifying photophysical and electrochemical properties (e.g., the rate of ET) of the Ir complex photocatalysis. Steric modification of the PNNP-type tetradentate ligand indeed substantiated the enhancement of the photocatalytic abilities arising from the robust photocatalyst. Capitalizing on the privileged characteristics, the



Scheme 1 This work: (a) Structures of (PNNP)Ir complexes and (b) Possible steric repulsion among chemical entities, and easier approach of CO₂ to a catalytic site.

^a Department of Chemistry, Graduate School of Science, Nagoya University, Chikusa, Nagoya 464-8602, Japan. E-mail: jieun@chem.nagoya-u.ac.jp

^b Institute for Materials Chemistry and Engineering, Kyushu University, Fukuoka 819-0395, Japan.

^c Toyota Central R&D Laboratories, Inc., Nagakute 480-1192, Japan.

^d Integrated Research Consortium on Chemical Science (IRCCS), Nagoya University, Chikusa, Nagoya 464-8602, Japan. E-mail: saito.susumu@f.mbox.nagoya-u.ac.jp

† Electronic Supplementary Information (ESI) available. See

scale-up design of the reaction considerably enhanced the catalytic performance to give a total TON of over 10400, which is superb and benchmark photocatalytic activity among self-photosensitized mononuclear molecular catalysts.

Photocatalytic reduction of CO₂ was examined by photoirradiation ($\lambda \geq 400$ nm) on a mixture solution of dimethylacetamide (DMA) and H₂O containing **1–4** under a CO₂ atmosphere in the presence of a sacrificial electron donor, 1,3-dimethyl-2-phenyl-2,3-dihydro-1*H*-benzo[*d*]-imidazole (BIH) or triethanolamine (TEOA). In all the cases, CO₂ reduction occurred, giving the products, HCO₂H, CO and H₂ (Table 1). In the reaction systems with BIH (Fig. 1a and Fig. S1, ESI[†]), their reactivities (>500 of TONs at 48 h) over all the (PNNP)Ir photocatalysts are superior to the previous results,^{6–9} where ≤ 265 (at 250 h) of TONs were achieved using mononuclear self-photosensitized Ir catalysts (Table S1, ESI[†]). Hydride ligands in (PNNP)Ir complexes work as an H-donor in the secondary coordination sphere to allow CO₂ insertion, leading to a formate product.¹³ Lower reducibility of **2** was observed with the $\text{TON}_{\text{HCO}_2\text{H}} = 543$, $\text{TON}_{\text{CO}} = 116$ and $\text{TON}_{\text{H}_2} = 1$ after 48 h photoirradiation, whereas the reactivity much increased with **4** in its well-purified form: after 48 h irradiation, HCO₂H, CO and H₂ were produced with the TONs of 2267, 532 and 5, respectively.

The sacrificial electron donor was next changed to TEOA from BIH. While the use of BIH ($E_{\text{ox}} = 0.21$ V vs SCE)^{12a} gave moderately high TONs, the reaction also proceeded with commercially available TEOA, which has a more positive one-electron oxidation potential ($E_{\text{ox}} = 0.68$ V vs SCE) with a weaker reducing ability. Whereas the TONs lowered with TEOA, the tendency (HCO₂H selectivity and the order of catalytic activity of **1–4**) towards photocatalytic CO₂ reduction resembles that with BIH; the highest TON and HCO₂H selectivity was obtained with **4** (Fig. S2, ESI[†]). Control experiments revealed that the Ir complex, electron donor and CO₂ are all needed for efficient photocatalytic CO₂ reduction (Fig. S3, ESI[†]). The quantum efficiency was determined to be $\sim 19\%$,¹⁴ together with 84% selectivity towards HCO₂H formation when the reaction solution of **4** was irradiated at $\lambda_{\text{ex}} = 400$ nm (light intensity = 2.07×10^{-9} einstein s⁻¹) with TEOA under a CO₂ atmosphere (Fig. S4, ESI[†]). A ¹³C-labeling experiment was also performed using a ¹³CO₂-saturated mixture of DMA-*d*₉/H₂O/TEOA (9:1:2, v/v/v), indicating that HCO₂H is from CO₂ gas (Figs. S5,S6, ESI[†]).

To ascertain the overwhelming robustness of the Ir complex photocatalyst derived from **4**, TEOA was further focused on

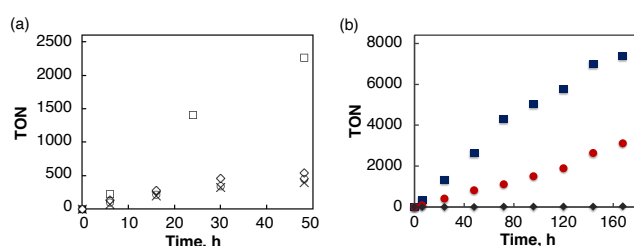


Fig. 1 (a) Time course plots of HCO₂H obtained in the photocatalytic CO₂ reduction with a catalytic amount (20 μM) of [**1** (x), **2** (◇), **3** (○) and **4** (□)] in a CO₂-saturated mixture of DMA:H₂O (9:1, v/v; 4 mL) and BIH (0.2 M) under photoirradiation ($\lambda \geq 400$ nm) at 298 K. (b) Time course plots of products [HCO₂H (blue), CO (red) and H₂ (black)] produced in the photocatalytic reduction of CO₂ in a CO₂-saturated mixture of DMA/H₂O (9:1, v/v; 4 mL) containing **4** (20 μM) and BIH (0.25 M) under photoirradiation ($\lambda \geq 400$ nm). The reaction vessel was scaled up from 8 mL (a) to 35 mL (b).

since it has been considered as a likely deactivating agent during photocatalysis.⁸ ESI-MS measurements before and after the reaction indicated that the lifetime of the photocatalyst elongated by mitigating its degradation through the insertion of a bulky ligand. After 24 h light irradiation to a CH₃CN/TEOA (5:1, v/v) solution of **2**, an original peak of **2** ($m/z = 805.3150$) was diminished, accompanied by the appearance of a new peak ($m/z = 809.3471$), which would be the complex with the one pyridine ring fully hydrogenated (Fig. S7, ESI[†]).⁷ Considering that the photocatalytic reactions with **2** reached a plateau shortly, the converted catalyst of **2** has low stability or reactivity. In contrast, the ESI-MS spectrum of **4** after the CO₂ photoreduction remained almost identical to that of the initial state with the base peak at 1041 m/z assignable to **4** (Fig. S8, ESI[†]). The attachment of OCO(O(CH₂)₂N[(CH₂)₂OH]₂)¹⁵/TEOA to **4**, and dimerization of **4**⁶ could not be assigned by ESI-MS. These results indicate that the mesityl moiety significantly decelerated the reduction of a pyridine of the bpy to piperidine, weakened the interaction of the Ir center with sacrificial electron donors, and enhanced the robustness of the photocatalyst.

Since **4** was highly robust toward light judging from the attenuated catalyst deactivation, reaction optimization was further attempted with **4**. Scaling up volumes of the reaction vessel (from 8 mL to 35 mL) led to sufficient CO₂ concentration inside the vessel, reproducing the photocatalytic reaction. The manipulation resulted in a continuous increase of TONs over 168 h photoirradiation to achieve the total TON > 10400 ($\text{TON}_{\text{HCO}_2\text{H}} = 7373$ and $\text{TON}_{\text{CO}} = 3114$) and the TOF > 62 h⁻¹ ($\text{TOF}_{\text{HCO}_2\text{H}} = 44$ and $\text{TOF}_{\text{CO}} = 18$) with 70% selectivity for HCO₂H formation (Fig. 1b and Table S1, ESI[†]). The highest TON (TON_{CO}

Table 1 Photocatalytic CO₂ reduction using Ir photocatalysts ($\lambda \geq 400$ nm) in 48 h and their physical properties

Entry	[Ir]	TONs with BIH ^a			TONs with TEOA ^b			λ_{abs} , nm	ϵ , M ⁻¹ cm ⁻¹	λ_{em} , nm	E_{red} , V vs SCE	E_{red}^* , V vs SCE	τ , ns	λ , ^c eV
		HCO ₂ H	CO	H ₂	HCO ₂ H	CO	H ₂							
1	1	399	294	2	17	21	<1	392	1722	587	-1.22	1.47	100	0.96
2	2	543	116	1	33	11	<1	396	1760	555	-1.22	1.33	160	0.85
3	3	449	97	4	45	18	1	384	2066	540	-1.30	1.33	82	0.89
4	4	2267	532	5	97	52	4	400	2160	562	-1.22	1.32	173	0.90

^a [Ir], 20 μM in a CO₂-saturated DMA:H₂O (9:1, v/v) containing BIH (0.2 M). ^b [Ir], 100 μM in a CO₂-saturated DMA:H₂O:TEOA (9:1:2, v/v/v). ^c Reorganization energy in excited-state electron transfer (ET) reactions.

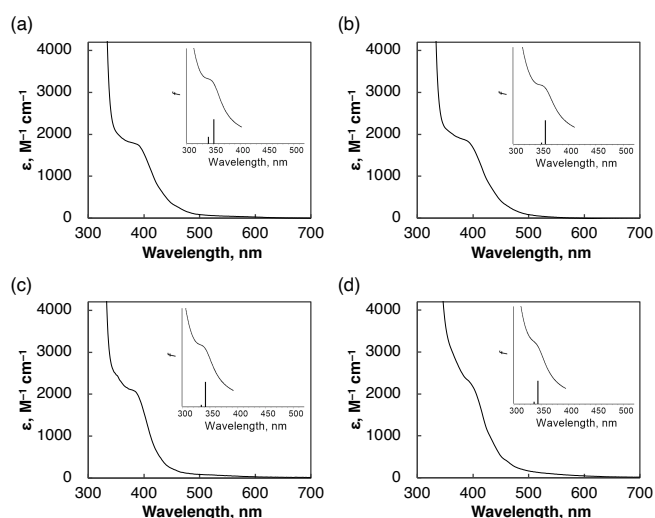


Fig. 2 UV-vis spectra of Ir complexes [(a) **1**, (b) **2**, (c) **3** and (d) **4**] (0.1 mM) in a deaerated DMA/H₂O (9:1, v/v) solution. Insets show simulated absorption spectra obtained from the TD-DFT calculations at the ωB97XD level of theory.

= 33000; CO: 66 nmol) was achieved at a 1 nM concentration of a Ru complex reported by Webster, Delcamp, Papish, and co-workers; however, the reaction reached a plateau on a micromolar scale to give the TON_{CO} of 55 (0.011 mmol with 100 μM of the Ru complex at 20 h).¹⁶ In contrast, the total TON of >10400 was achieved at a 20 μM concentration of **4**, producing a 0.590 mmol of HCO₂H and a 0.249 mmol of CO. CO₂ photoreduction also proceeded using a solar simulator to give the total TON of > 5200 after 120 h photoirradiation (Fig. S9, ESI[†]). Although the solar simulator covers a broad range of light from UV to NIR, the robustness of the catalyst was kept uniformly with different wavelengths.

A vault of photophysical properties of Ir complexes was further examined to elucidate substituent effects. UV-vis absorption (Fig. 2) and emission spectra (Fig. S10, ESI[†]) of the Ir complexes **1–4** shared similar features of strong absorption bands below 390 nm with the associated absorption parameters: maximum absorption wavelength (λ_{abs}), molar extinction coefficient (ϵ), and maximum fluorescence emission wavelength (λ_{em}) (Table 1). The electronic transitions of (PNNP)Ir were investigated using the time-dependent density functional theory (TD-DFT) method. The calculated excitation wavelengths and oscillator strengths for selected transitions are listed in Table S2, and the absorption spectra obtained by broadening the calculated oscillator strengths with Gaussian functions are depicted in Fig. 2. The computed results were consistent with experimental observation. The transitions in the visible-light region mainly arise from the MLCT transition from the d_{π} (t_{2g}) orbitals of Ir to the π^* orbitals of bpy.

To study the excited states of **1–4** involved in the photocatalytic CO₂ reduction, sub-nanosecond laser-induced transient absorption measurements based on a Randomly-Interleaved-Pulse-Train (RIPT) method¹⁷ were conducted using a commercially available instrument (picoTAS, Unisoku). Upon photoexcitation on a deaerated DMA solution of an Ir complex, a new absorption band at $\lambda_{\text{max}} = 480$ nm for **1*** and **2*** (Fig. 3), and 500 nm for **3*** (* denotes the excited state) were observed,

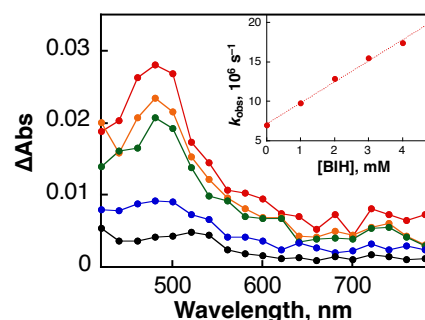


Fig. 3 (a) Transient absorption spectral changes [red (2 ns); orange (20 ns); green (50 ns); blue (200 ns); black (500 ns)] after sub-nanosecond laser excitation at 355 nm in a deaerated DMA solution containing **2** (2.0 mM) at 298 K. (b) Plot of k_{obs} vs concentration of BIH in a DMA solution at 298 K.

which can be assigned to the triplet (T_1) excited state. It is known that intersystem crossing processes from the singlet (S_1) to the T_1 excited state are extremely rapid because of strong spin-orbit coupling.¹⁸ From the decay time profile of absorbance at 480 nm, the lifetime of the T_1 of **2** was determined to be $\tau = 160$ ns at 298 K. Similarly, the lifetimes of the T_1 state of **1** and **3** were determined to be 100 and 82 ns (Table 1). Compared with the τ of **4** (173 ns),^{12a} their structural relaxation to the ground states (S_0) is faster owing to conformational flexibility endowed with their smaller sizes.

When BIH as an electron donor was added to a deaerated and photo-irradiated DMA solution of **2** devoid of mesityl groups from **4**, the decay of absorbance at 480 nm due to the T_1 excited state of **2** was more accelerated, and the decay rate constant (k_{obs}) increased linearly with increasing concentration of BIH (Fig. 3, inset). The ET occurred from BIH to the T_1 excited state of **2** (**2***). The rate constant of the ET (k_{et}) was determined from the slope of the linear plot of k_{obs} vs concentration of BIH to be $2.9 \times 10^9 \text{ M}^{-1} \text{ s}^{-1}$ at 298 K. The k_{et} due to ET from BIH or TEOA to [Ir]* of **1–4** were also determined, where the k_{et} decreases in the order of **1** > **2** > **3** > **4**^{12a} (Figs. S11–S15, ESI[†]). These results suggest that both TEOA and BIH could approach more approximate to Ir complexes for ET as their bulkiness decreases. The k_{et} values of ET from various ferrocene and methoxybenzene derivatives to the T_1 state of **1–3** roughly showed similar trends (Table S3, Figs. S16–S33, ESI[†]). The plot of $\log k_{\text{et}}$ as a function of the one-electron oxidation potentials of the electron donors (E_{ox} , vs SCE) (Fig. S34, ESI[†]) exhibits the expected behavior as expressed by the Marcus equation of intermolecular ET^{19,20} and the best fit in Fig. S34 gives E_{red}^* values of 1.47(1) V, 1.33(1), 1.33(1) V and 1.32(1) V (vs SCE) as well as λ of 0.96(4) eV, 0.85(4), 0.89(4) and 0.90(4) eV^{12a} for **1***–**4***, respectively, along with a k_{diff} of $7.0 \times 10^9 \text{ M}^{-1} \text{ s}^{-1}$ (Table 1). The substituent of the P atom, rather than of bpy, affects more substantially the E_{red}^* value of the T_1 state and structural reorganization from **1*–4*** to their one-electron reduced species.

Electrochemical properties of **1–4** are almost similar to one another. Cyclic voltammetry (CV) measurements of **1–3** were conducted in a DMA solution under Ar (Table 1 and Fig. S35, ESI[†]), giving quasi-reversible redox couples similar to that of

4.12a The catalytic current growth was uniformly given under a CO₂ atmosphere. Reduction potentials of **1**, **2**, and **4** are almost the same (−1.22 V vs SCE) and that of **3** is slightly more negative (−1.30 V vs SCE). DFT calculations (Fig. S36, ESI[†]) indicated that the one-electron reduction could be attributed to the redox couple of the ligand of (PNNP)Ir, [P(bpy)P/P(bpy[−])P]. Above all, introducing the bulky substituents at the bpy and P atom showed a remarkable increase in the photostability of **4** compared with **1–3** (Fig. 1), where all the photophysical and electrochemical results indicate that the “steric” is more critical than “electronic” to virtually accelerate photocatalytic CO₂ reduction with a long lifespan.

In summary, we have demonstrated the superb effects of bulky substituents on photocatalytic abilities of (PNNP)Ir complexes. Bulkier substituents in bpy (R¹: H < tBu < Mes) and phosphine (R²: *i*-Pr < Cy) moieties stabilized the catalyst by sufficient steric hindrance,^{6,21} and improved its durability to give higher TON and TOF. Ultimately, Ir complex **4** ([**4**]₀ = 20 μM) reduces CO₂ to achieve TON_{red} = 149 with TEOA and TON_{red} >10400 (HCO₂H, 0.590 mmol; CO, 0.249 mmol) with BIH, which is the highest and the most scalable among self-photosensitized, mononuclear Ir catalysts for CO₂-reduction. ESI-MS measurements indicated that the reduction of pyridine to piperidine during the photocatalysis was significantly decelerated by the introduction of mesityl groups at the bpy moiety. Photophysical and electrochemical properties have been investigated and these values indicate that the steric effect is more essential than electronic effects to facilitate overall steps through the CO₂ photoreduction. The present study has thus provided new insights into the development of efficient catalysts for CO₂ reduction reactions.

Conflicts of interest

There are no conflicts to declare.

Acknowledgments

This work was supported by the Asahi Glass Foundation (Step-up-grant to S.S.), the Japanese Society for the Promotion of Science (Grant-in-Aid for Scientific Research (B) (no. 19H02713 to S.S.), Early-Career Scientists (no. 21K14642 to J. J.), and a Research Fellowship for Young Scientists (no. 21J14046 to K. K.)), and partially by the Ministry of the Environment of the Government of Japan.

Notes and references

- (a) A. Behera, A.-K. Kar and R. Srivastava, *Mater. Horiz.*, 2022, **9**, 607–639; (b) Y.-H. Luo, L.-Z. Dong, J. Liu, S.-L. Li and Y.-Q. Lan, *Coord. Chem. Rev.*, 2019, **390**, 86–126; (c) R. Francke, B. Schille and M. Roemelt, *Chem. Rev.*, 2018, **118**, 4631–4701.
- (a) R. Cauwenbergh and S. Das, *Green Chem.*, 2021, **23**, 2553–2574; (b) Y. Yamazaki, H. Takeda and O. Ishitani, *J. Photochem. Photobiol. C*, 2015, **25**, 106–137; (c) S. Fukuzumi, Y.-M. Lee, H. S. Ahn and W. Nam, *Chem. Sci.*, 2018, **9**, 6017–6034.
- (a) M. Rumayor, A. Dominguez-Ramos and A. Irabien, *Appl. Sci.*, 2018, **8**, 914; (b) J. Huang and L. Wang, *Electrochim. Acta*, 2019, **319**, 569–576.
- (a) Z. Chen, H. Zhang, P. Guo, J. Zhang, G. Tira, Y. J. Kim, Y. A. Wu, Y. Liu, J. Wen, T. Rajh, J. Niklas, O. G. Poluektov, P. D. Laible and E. A. Rozhkova, *J. Am. Chem. Soc.*, 2019, **141**, 11811–11815; (b) S. Zhang, Z. Xia, Y. Zou, F. Cao, Y. Liu, Y. Ma and Y. Qu, *J. Am. Chem. Soc.*, 2019, **141**, 11353–11357; (c) R. Kuriki, T. Ichibha, K. Hongo, D. Lu, R. Maezono, H. Kageyama, O. Ishitani, K. Oka and K. Maeda, *J. Am. Chem. Soc.*, 2018, **140**, 6648–6655.
- (a) C. Finn, S. Schnittger, L. J. Yellowlees and J. B. Love, *Chem. Commun.*, 2012, **48**, 1392–1399; (b) A. M. Appel, J. E. Bercaw, A. B. Bocarsly, H. Dobbek, D. L. DuBois, M. Dupuis, J. G. Ferry, E. Fujita, R. Hille, P. J. A. Kenis, C. A. Kerfeld, R. H. Morris, C. H. F. Peden, A. R. Portis, S. W. Ragsdale, T. B. Rauchfuss, J. N. H. Reek, L. C. Seefeldt, R. K. Thauer and G. L. Waldrop, *Chem. Rev.*, 2013, **113**, 6621–6658; (c) R. Francke, B. Schille and M. Roemelt, *Chem. Rev.*, 2018, **118**, 4631–4701; (d) R.-R. Rodrigues, C.-M. Boudreaux, E.-T. Papish and J.-H. Delcamp, *ACS Appl. Energy Mater.*, 2019, **2**, 37–46;
- S. Sato, T. Morikawa, T. Kajino and O. Ishitani, *Angew. Chem., Int. Ed.*, 2013, **52**, 988–992.
- S. Sato and T. Morikawa, *ChemPhotoChem*, 2018, **2**, 207–212.
- (a) R. O. Reithmeier, S. Meister, B. Rieger, A. Siebel, M. Tschurl, U. Heiz and E. Herdtweckd, *Dalton Trans.*, 2014, **43**, 13259–13269; (b) R. O. Reithmeier, S. Meister, A. Siebel and B. Rieger, *Dalton Trans.*, 2015, **44**, 6466–6472.
- A. Genoni, D. N. Chirdon, M. Boniolo, A. Sartorel, S. Bernhard and M. Bonchio, *ACS Catal.*, 2017, **7**, 154–160.
- (a) T. Miura, I. E. Held, S. Oishi, M. Naruto and S. Saito, *Tetrahedron Lett.*, 2013, **54**, 2674–2678; (b) T. Miura, M. Naruto, K. Toda, T. Shimomura and S. Saito, *Sci. Rep.*, 2017, **7**, 1586; (c) S. Yoshioka, S. Nimura, M. Naruto and S. Saito, *Sci. Adv.*, 2020, **6**, eabc0274; (d) B. Grømer, S. Yoshioka, S. Saito, *ACS Catal.*, 2022, **12**, 1957–1964.
- (a) S. Oldenhof, J. I. van der Vlugt and J. N. H. Reek, *Catal. Sci. Technol.* 2016, **6**, 404–408; (b) H. Li, X. Wang, F. Huang, G. Lu, J. Jiang and Z.-X. Wang, *Organometallics*, 2011, **30**, 5233–5247.
- (a) K. Kamada, J. Jung, T. Wakabayashi, K. Sekizawa, S. Sato, T. Morikawa, S. Fukuzumi and S. Saito, *J. Am. Chem. Soc.*, 2020, **142**, 10261–10266; (b) K. Kamada, H. Okuwa, T. Wakabayashi, K. Sekizawa, S. Sato, T. Morikawa, J. Jung and S. Saito, *Synlett* 2022, **33**, A–E (DOI: 10.1055/a-1709-0280).
- (a) S. Oldenhof, J. I. van der Vlugt and J. N. H. Reek, *Catal. Sci. Technol.*, 2016, **6**, 404–408; (b) J. S. Timothy, E. D. Graham, H. C. Robert and H. Nilay, *J. Am. Chem. Soc.* 2011, **133**, 9274–9277.
- C. G. Hatchard and C. A. Parker, *Proc. R. Soc. London, Ser. A*, 1956, **235**, 518–536.
- T. Morimoto, T. Nakajima, S. Sawa, R. Nakanishi, D. Imori and O. Ishitani, *J. Am. Chem. Soc.*, 2013, **135**, 16825–16828.
- S. Das, R. R. Rodrigues, R. W. Lamb, F. Qu, E. Reinheimer, C. M. Boudreaux, C. E. Webster, J. H. Delcamp and E. T. Papish, *Inorg. Chem.*, 2019, **58**, 8012–8020.
- T. Nakagawa, K. Okamoto, H. Hanada and R. Katoh, *Opt. Lett.*, 2016, **41**, 1498–1501.
- (a) R. Ballardini, G. Varani, M. T. Indelli and F. Scandola, *Inorg. Chem.*, 1986, **25**, 3858–3865; (b) X.-Y. Liu, Y.-H. Zhang, W.-H. Fang and G. Cui, *J. Phys. Chem. A*, 2018, **122**, 5518–5532.
- G. J. Kavarnos, *Fundamentals of Photoinduced Electron Transfer*; Wiley-VCH: New York, 1993.
- (a) R. A. Marcus, *Annu. Rev. Phys. Chem.* 1964, **15**, 155–196; (b) R. A. Marcus, *Angew. Chem., Int. Ed. Engl.* 1993, **32**, 1111–1121.
- M. D. Sampson, A. D. Nguyen, K. A. Grice, C. E. Moore, A. L. Rheingold and C. P. Kubiak *J. Am. Chem. Soc.*, 2014, **136**, 5460–5471.